Master's Thesis of Science
in Food Science and Biotechnology

Structural and mechanistic analyses of the DNA repair nuclease SbcD from the foodborne pathogen *Staphylococcus aureus*

식품매개 병원균 황색포도상구균 유래 DNA 수선 핵산가수분해효소 SbcD의 구조 및 기작 분석

August 2020

Food Science and Biotechnology Major
Department of Agricultural Biotechnology
The Graduate School
Seoul National University

Jinwook Lee

석사학위논문

Structural and mechanistic analyses of the DNA repair nuclease SbcD from the foodborne pathogen *Staphylococcus aureus*

지도교수 하 남 출

이 논문을 석사학위논문으로 제출함

2020년 8월

서울대학교 대학원

농생명공학부 식품생명공학전공

이 진 욱

이진욱의 석사학위논문을 인준함
2020년 8월

위원장	최 상 호	(인)
부위원장	하 남 출	(인)
위원	장 판 식	(인)

Abstract

Staphylococcus aureus is a major foodborne pathogen causing food poisoning in humans. To prevent infection of *S. aureus*, food must be sterilized by proper treatments during food processing, such as heating, ultraviolet light radiation, and hypochlorous acid (HOCl) treatment. These treatments give damages to the bacterial DNA, for instance, DNA double-strand break (DSB), thereby inhibition of protein expression, leading to the death of the bacteria. If bacteria have robust DNA repair systems, the bacteria could have a strong resistance to the treatments. In *S. aureus*, a SbcCD complex was known as an essential component of the DSB repair system. The SbcCD complex recognizes and cleaves the DNA ends in DSB by ATP-dependent endo- and exonuclease activities as the initial step of the DNA repair. The SbcD component consists of a nuclease, capping, and helix-loop-helix (HLH) domain. The structural studies of SbcD have focused on Gram-negative bacteria, and there is no structural information of SbcD in Gram-positive bacteria to date. Moreover, it remains to be elucidated the action mechanism at the molecular level of bacterial SbcCD complex. Here, I studied the nuclease and capping domain of SbcD from the Gram-positive bacteria *S. aureus.* The protein was overexpressed and purified, and its crystals suitable for the structural study were obtained. X-

ray diffraction dataset was collected at a resolution of 2.9 Å, and the structure of the SbcD nuclease and capping domain (NCD) was determined by X-ray crystallography. Two manganese ions were found at the active site of SbcD and were coordinated by seven residues, sharing with SbcD of *E. coli*. The nuclease activity test with the SbcD-NCD protein exhibited the endonuclease activity on supercoiled DNA, and the exonuclease activity on linear DNA and nicked DNA. Combined with the structural and functional results, a molecular mechanism on how the SbcCD complex regulates these activities in repairing the DSB was proposed. Since SbcD is essential in the survival of *S. aureus* like other bacteria from DNA damage stresses, this study will provide a potential in controlling foodborne pathogen *S. aureus* by suppressing the resistance to food sterilization processes.

Keyword: Staphylococcus aureus, foodborne pathogen, DNA double-strand breakage, DNA repair, Nuclease, crystal structure

Student Number: 2018-22430

Contents

List of Figures

List of Tables

I. Introduction

Staphylococcus aureus is a major foodborne pathogen that causes various epidermal infections, food poisoning, pneumonia, meningitis, and sepsis in humans. *S. aureus* produces multiple virulence factors, which include surface-associated adhesions, exo-proteins, and secreted toxins, contributing to the pathogenesis of *S. aureus* [1-3].

The precise replication and proper maintaining of the genome are essential in all living creatures, including bacteria and humans [4]. However, various physical, chemical, and biochemical stresses can damage the DNA in many different ways, which could lead to genomic alterations from point mutations to abnormal chromosome structures. The damaged DNA regions are detected and repaired by diverse proteins in different mechanisms [5-7]. Of these, the complex consisting of the nuclease Mre11 and the ATPase Rad50 in eukaryotes promptly detect and process DNA double-strand breaks (DSBs), hairpins, and other abnormal terminal DNA structures [8, 9]. The complex is highly conserved throughout the life kingdoms, and bacteria have the SbcCD complex consisting of the nuclease component SbcD and the ATPase SbcC as the homolog of the Mre11-Rad50 complex [10]. In yeast, the Mre11-Rad50 complex was characterized as the main response factor for the repair of DSBs involving Non-homologous end joining

(NHEJ), Homologous Recombination (HR), and maintenance of telomere [8, 11-13].

SbcCD recognizes the abnormal DNA structure, and processes the blocked or obstructed DNA ends by exhibiting the 3’ to 5’ exonuclease activity, and cutting the DNA near protein-bound DNA ends [14]. The complex can also cleave the hairpin structures at the 5’ of the DNA loop with endonuclease activity [15, 16]. Recently, it was reported that SbcCD exhibits intrinsic and robust endonuclease activity and can shorten the DNA ends further through an ATP-dependent binary endonuclease activity unlike the eukaryotic Mre11-Rad50 complex [17]. Many different action modes have been found in SbcCD. The complex cleaves the opposing strands of DNA by two chemically distinct nuclease reactions [18, 19].

The SbcC component consists of an ATP-binding cassette (ABC) type nucleotide-binding domain and a flanking 10-50 nm long coiled-coil insertion containing a zinc-hook motif for dimerization [20, 21]. Thus the SbcC dimer exhibited a V-shaped structure, which included the nucleotide-binding domain at both open ends of the V-shaped structure [21-23]. The SbcD component consists of a nuclease domain, a capping domain, a linker, and a helix-loop-helix domain. SbcD also forms a dimer via the nuclease domain, and the SbcD dimer makes the complex with SbcC via the nucleotide-binding domain of SbcC, closing the V-shape the structure [24].

Interestingly, the SbcCD complex shows a similar structural architecture to the structural maintenance of chromosomes (SMC) protein functioning in the DNA compaction, which is different from the DNA repair function of SbcCD complex [25-27].

Several crystal structures of the components of the SbcCD complex have been determined. However, the action mechanism at the molecular level still needs to be elucidated. Furthermore, most studies have been performed in Gram-negative bacteria *Escherichia coli*, although the sequence similarity to the Gram-positive bacteria is limited. Here, I studied the nuclease and capping domain of SbcD from the Gram-positive bacteria *S. aureus*. The protein was overexpressed and purified, and its protein crystals were obtained. X-ray diffraction dataset was collected, and the structure of the SbcD nuclease and capping domain (NCD) was determined by X-ray crystallography. Ensuing biochemical study with various DNA substrates, combined with the structure, provides the mechanistic roles of the SbcD NCD.

II. Experimental Procedures

II-1. Construction for the protein expression

The gene coding for the nuclease and capping domain (NCD) (residues 1-320) of SbcD (NCBI reference sequence: BAB57507.1) was amplified from the genomic DNA from *S. aureus* Mu50 using PCR. The primer sequences used for PCR are described in Table 1. The PCR products were digested by restriction enzymes *Nco*I and *Xho*I and inserted into the two enzyme sites in the pProEx-Hta vector (Invitrogen, USA). The resulting pProEx-Hta-SbcD-NCD vector contains the 6xHis-tag at the N-terminus of the protein for purification and a TEV protease cleavage site for removing the tag (Table 1).

II-2. Protein overexpression and purification

To express the SbcD-NCD protein, the recombinant plasmid pProEx-Hta-SbcD-NCD was transformed into *E. coli* BL21 (DE3) cells. The cells were cultured in 3.0 L LB medium supplemented with 100 μg/mL ampicillin, at 37℃ until OD_{600} value reached 0.8. 0.5 mM IPTG was added to the culture medium to induce the SbcD NCD protein. The cells were further cultured at 30℃ for 8 hours and were harvested by centrifugation at 1400xg for 7 min at 4℃. The cell pellet was resuspended with 50 ml of lysis buffer containing 20 mM Tris (pH 8.0), 150 mM NaCl and 2 mM β-mercaptoethanol. A

sonicator was employed to disrupt the cells, and then the cell debris was removed by centrifugation at 20000xg for 30 min at 4℃.

Ni-NTA agarose resin (1 ml; Qiagen, Germany) was mixed with 50 ml of the cell lysate solution and gently rolled in a column for 50 min at 4℃. The resin was washed with 250 ml of a buffer containing 20 mM Tris (pH 8.0), 150 mM NaCl, 20 mM imidazole (pH 8.0) and 2 mM β-mercaptoethanol, and then the protein was subsequently eluted with 25 ml of a buffer containing 20 mM Tris (pH 8.0), 150 mM NaCl, 250 mM imidazole (pH 8.0), and 2 mM β-mercaptoethanol were treated with a recombinant TEV protease for 14 hours at the room temperature to cleave the 6xHis-tag, where 0.5 mM EDTA and 2 mM TCEP were added to the reaction solution.

The fractions of the protein were pooled and were further purified with the anion exchange chromatographic column (Hitrap Q, GE Healthcare, USA) by applying a gradient from 0 mM to 1 M NaCl. The protein was eluted in a range of 400-450 mM NaCl. The pooled fractions were further purified using a gel filtration chromatographic column (HiLoad^{TM} 26/610 Superdex^{TM} 200pg; GE Healthcare, USA), which was pre-equilibrated with 20 mM Tris buffer (pH 8.0) containing 300 mM NaBr and 2 mM β-mercaptoethanol. The resulting protein solution was concentrated to 7 mg/ml using a Vivaspin centrifugal concentrator (30 kDa molecular-weight

cutoff; Millipore, USA), and stored frozen at -80℃ until use.

II-3. Size exclusion chromatography-multi angle light scattering (SEC-MALS) of SbcD-NCD

The SEC-MALS experiment was performed to examine the oligomeric state of SbcD-NCD. Size exclusion chromatography using Superdex-200 10/300 GL (GE Healthcare) gel filtration column was performed in Wyatt DAWN HELIOS II MALS system. The SbcD-NCD protein was loaded to the gel filtration column and then pre-equilibrated with a buffer solution containing 20 mM Tris-HCl (pH 8.0), 150 mM NaCl, and 2 mM β-mercaptoethanol. The data were analyzed by the ASTRA 6 software (Wyatt, USA).

II-4. Crystallization

One mM $MnCl_2$ was added to the protein to improve the stability of SbcD-NCD. An automated crystal screening device MOSQUITO was employed for initial crystallization trials of the SbcD-NCD protein at 14℃ with a sitting-drop vapor-diffusion method. Seven matrix screening solutions (MCSG 1T, 2T, 3T, 4T, PEG/RX, PEG/ION, and Hampton Research Crystal Screen) were selected. The protein solution (0.2 μl, 7 mg/ml) was mixed with a reservoir solution (0.2 μl) and then was equilibrated against 60 μl of

the reservoir solution in a 96-well crystallization plate. Plate-shaped crystals appeared under the reservoir solution containing 2% (v/v) Tacsimate^{TM} (pH 6.0) (Hampton Research, USA), 0.1 M Bis-Tris (pH 6.5), 18% (w/v) polyethylene glycol. The crystallization conditions were optimized with the hanging-drop diffusion method under a reservoir solution containing 2% (v/v) Tacsimate^{TM} (pH 6.0), 0.1 M Bis-Tris (pH 7.0), 18% (w/v) polyethylene glycol at 14℃. In the final optimization experiments, long rod-shaped crystals suitable for data collection were obtained in 3-5 days (Fig. 2) by mixing 1 μl of the protein solution (7 mg/ml) and 1 μl of the reservoir solution, and equilibration against 500 μl of the reservoir solution in a 15-well plate.

II-5. Data collection and Structural determination

For data collection under cryogenic conditions, the SbcD-NCD crystals were transferred to 2 μl of the viscous oil Paraton-N and incubated for 1 sec. Then crystals were flash-cooled in liquid nitrogen at -173℃ for data collection. The datasets were collected on ADSC quantum Q270 CCD detector in beamline 11C of Pohang Accelerator Laboratory, Republic of Korea, at a wavelength of 0.97942 Å. The program HKL-2000 was used to process, merge, and scale the diffraction datasets [28]. Table 2 describes the data-collection statistics. The structure of the SbcD-NCD was determined

using the molecular replacement method with MOLREP in the CCP4 package [29], using the *E. coli* SbcD structure (PDB code: 6s6v) as a model. The structure of the SbcD-NCD was built and refined using COOT and PHENIX refine software [30, 31].

II-6. Nuclease assays

The nuclease assays were performed to test the nuclease activity of SbcD-NCD. Linear DNA and nicked DNA were generated using restriction enzyme EcoRI and nicking endonuclease Nt.BstNBI from 2002 bp circular double-stranded DNA. DNA substrates (500 ng) with 10 μM SbcD-NCD were incubated at 37℃ for 60 min in buffer solution containing 20 mM Tris pH 8.0, 150 mM NaCl, 2 mM β-mercaptoethanol and 5 mM $MnCl_2$. Supercoiled DNA was cleaved with 10 μM SbcD-NCD at 37℃ for 1, 5, 15, 30, 60 min in buffer solution containing 20 mM Tris pH 8.0, 150 mM NaCl, 2 mM β-mercaptoethanol and 5 mM $MnCl_2$. Cleavage of nicked DNA was performed with 10 μM SbcD-NCD at 37℃ for 1, 5, 15, 30, 60 min in buffer solution containing 20 mM Tris pH 8.0, 150 mM NaCl, 2 mM β-mercaptoethanol and 5 mM $MnCl_2$. Images were analyzed using ImageJ software.

III. Result

III-1. SbcD overexpression and purification

The full-length SbcD from *S. aureus* was overexpressed in the pLIC vector *E. coli* expression system to investigate the structural and functional studies. Although a highly pure full-length SbcD protein was obtained by multiple chromatographic purification steps (Fig. 1), it was not successful in obtaining the crystals with the protein sample, unfortunately.

I next expressed the nuclease and capping domain (residues 1-320; NCD) of SbcD (Fig. 2) in the pProEx-Hta vector system (Invitrogen, USA) to increase the probability of obtaining the crystals. The recombinant SbcD-NCD protein contained the N-terminal the 6xHis-tag for the purification and the TEV protease cleavage site for removing the tag. Ni-NTA affinity chromatography was applied for the initial purification from the soluble lysate of the cultured *E. coli* cells. Then, the recombinant TEV protease treatment cleaved the 6xHis-tag from the SbcD-NCD. The addition of 0.5 mM EDTA and 2 mM TCEP to the reaction solution was required to increase the efficiency of the TEV protease treatment.

The protein was further purified using anion-exchange chromatography and size-exclusion chromatography. The final protein

sample was concentrated to 7 mg/ml, which was measured by Bradford assay, with a high purity of >95% on SDS-PAGE (Fig. 3). The protein band appeared in the molecular weight of 35 kDa on the SDS polyacrylamide gel, which is well matched to the theoretical value of SbcD-NCD (36.5 kDa). SEC-MALS result of SbcD-NCD showed that SbcD-NCD has a molecular weight of 36.1 kDa (Fig. 4) representing that SbcD-NCD is a monomeric state in solution.

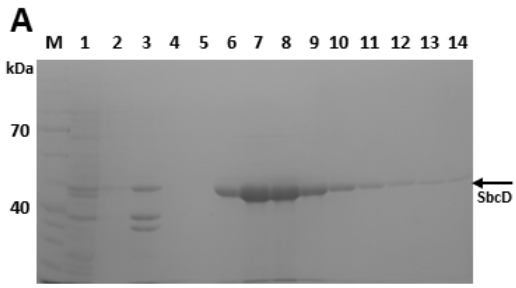

Lane 1 : Before induction
Lane 2 : Supernatant fraction
Lane 3 : Precipitant fraction
Lane 4 : Unbound fraction
Lane 5 : Washed fraction
Lane 6-14 : Eluted fraction

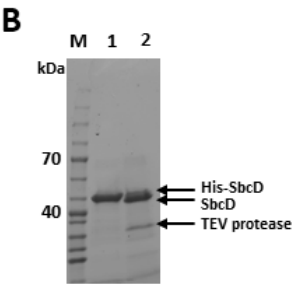

Lane 1 : Before TEV protease cleavage
Lane 2 : After TEV protease cleavage

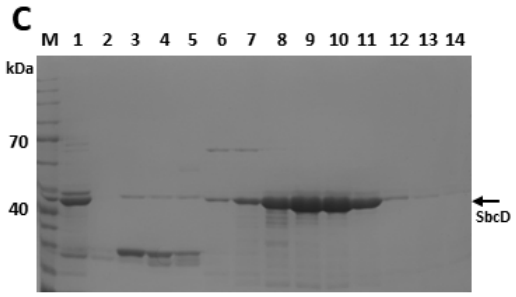

Lane 1 : Before anion exchange chromatography
Lane 2 : Q-column unbound fraction
Lane 3-5 : TEV protease
Lane 4-14 : Eluted fraction

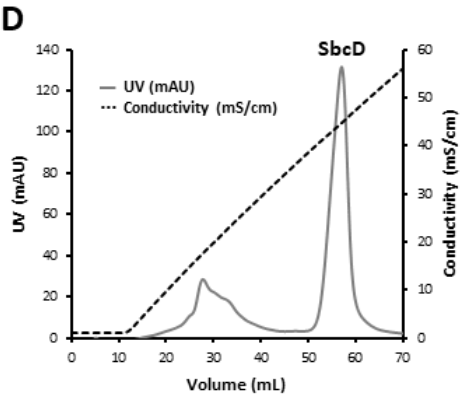

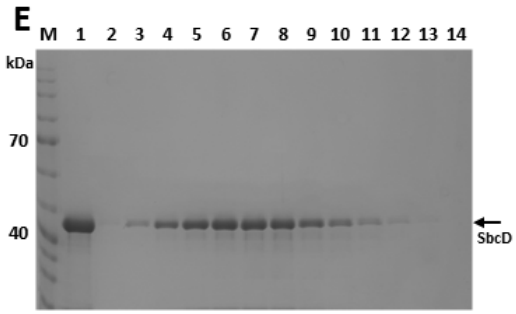

Lane 1 : Before size exclusion chromatography
Lane 2-14 : Eluted fraction

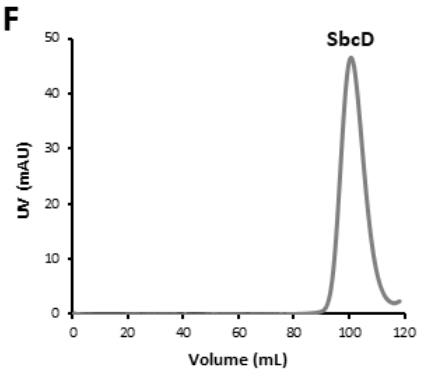

Figure 1. Purification profile of full-length SbcD

A. The SDS-PAGE profile of Ni-NTA affinity chromatography. Protein bands appear in the molecular weight of 43 kDa. **B.** The SDS-PAGE profile of 6xHis-tag cleavage by TEV protease. **C.** The SDS-PAGE profile of anion exchange chromatography. **D.** Diagram of UV and conductivity during anion exchange chromatography. **E.** The SDS-PAGE profile of size exclusion chromatography. **F.** Diagram of UV during size exclusion chromatography.

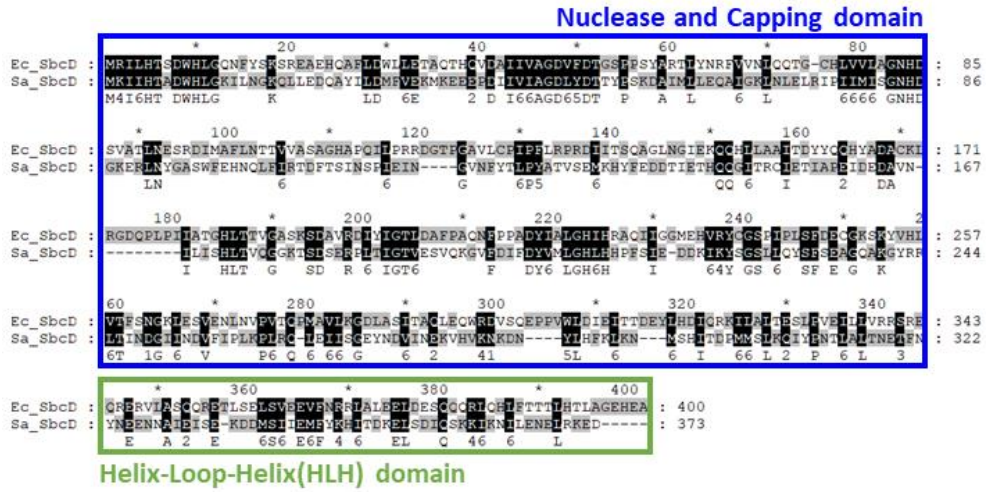

Figure 2. Sequence alignment of *S. aureus* SbcD with *E. coli* SbcD

A boxed area with the blue line is the nuclease and capping domain of SbcD.

Table 1. Production information of *S. aureus* SbcD-NCD

	SbcD-NCD
Source organism	*Staphylococcus aureus* Mu50
DNA source	Genomic DNA
Forward primer	GGCCCATGGCAAAAATTATACATACAG CAGAC
Reverse primer	GGCCTCGAGTCAAGTTTCATTCGTCAG CGC
Expression vector	pProEx-Hta
Expression host	*E. coli* BL21 (DE3)
Complete amino acid sequence of the construct produced	MSYYHHHHHHDYDIPTTENLYFQGAM AKIIHTADWHLGKILNGKQLLEDQAYIL DMFVEKMKEEEPDIIVIAGDLYDTTYPS KDAIMLLEQAIGKLNLELRIPIIMISGNH DGKERLNYGASWFEHNQLFIRTDFTSIN SPIEINGVNFYTLPYATVSEMKHYFEDD TIETHQQGITRCIETIAPEIDEDAVNILISH LTVQGGKTSDSERPLTIGTVESVQKGVF DIFDYVMLGHLHHPFSIEDDKIKYSGSLL QYSFSEAGQAKGYRRLTINDGIINDVFIP LKPLRQLEIISGEYNDVINEKVHVKNKD NYLHFKLKNMSHITDPMMSLKQIYPNTL ALTNET (The underlined residues are cleaved off by the TEV treatment).

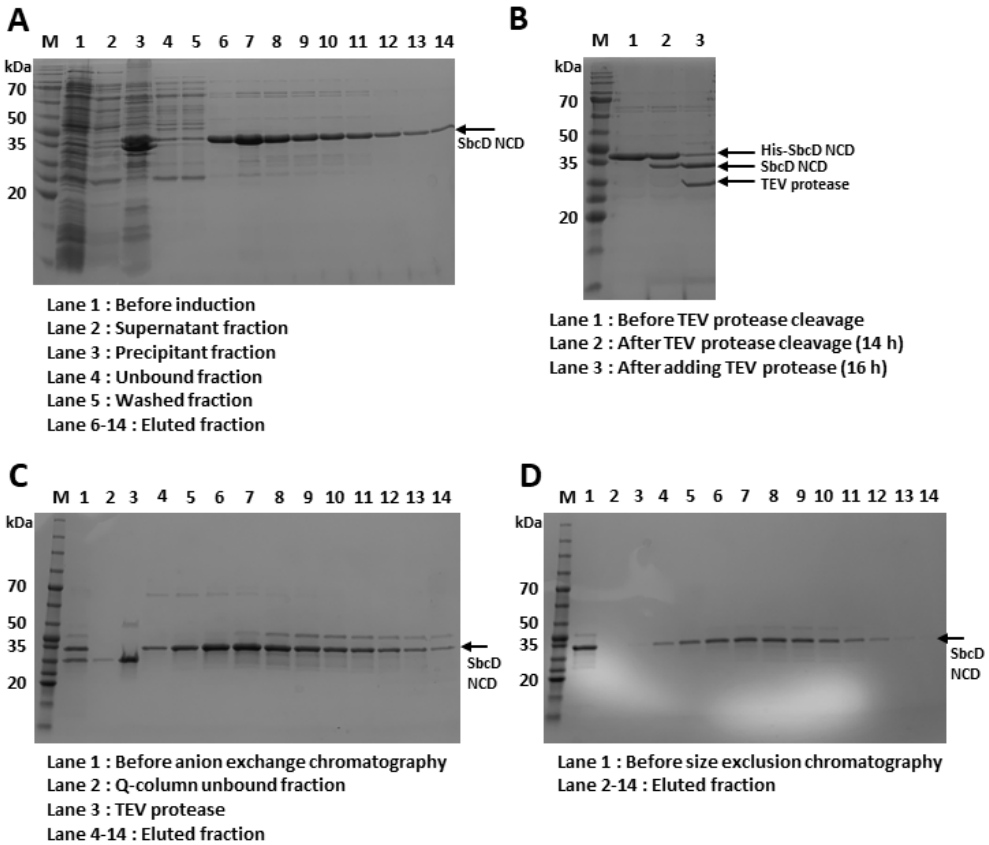

Figure 3. Purification profile of SbcD-NCD on SDS-polyacrylamide gel

The size marker proteins are presented in the left line (kDa). Protein bands appear in the molecular weight of 35 kDa. **A.** The SDS-PAGE profile of Ni-NTA affinity chromatography. **B.** The SDS-PAGE profile of 6xHis-tag cleavage using TEV protease. **C.** The SDS-PAGE profile of anion exchange chromatography. **D.** The SDS-PAGE profile of size exclusion chromatography.

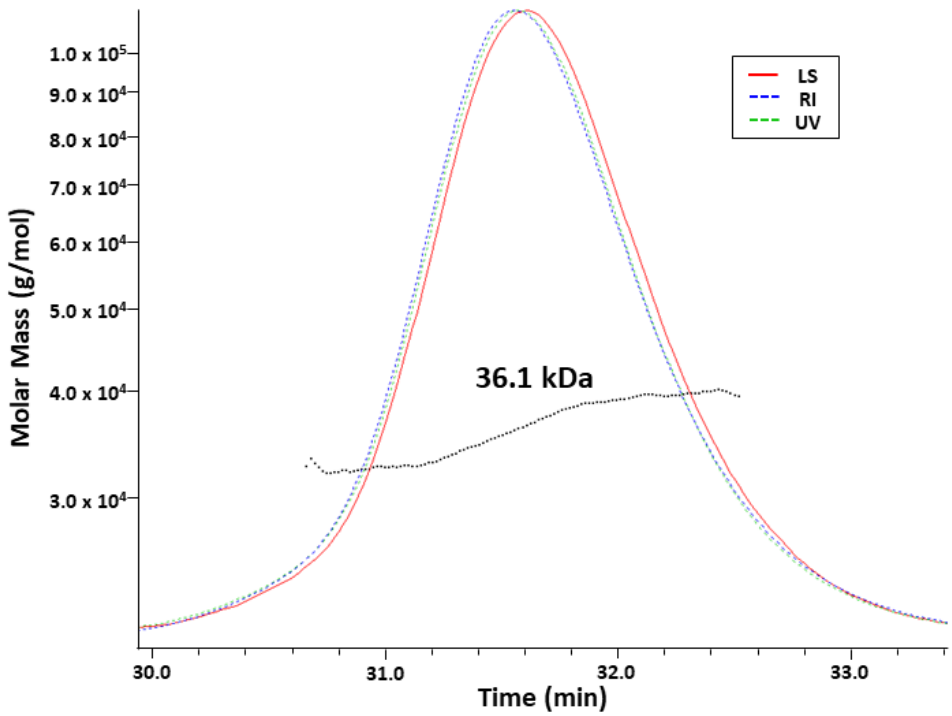

Figure 4. The SEC-MALS diagram of SbcD-NCD

Y-axis represents molar mass, which is determined using multi-angle light scattering (MALS; black dotted line). Protein concentrations were assessed by the light scattering (LS; red), the refractive index (RI; blue), and measuring the absorbance at 280 nm (UV; green). The X-axis represents elution time during size-exclusion chromatography.

III-2. Crystallization and structural determination of SbcD-NCD

To improve the stability and crystallization efficiency of SbcD, 1 mM $MnCl_2$ was added to the protein. Previous structural study with *E. coli* SbcD showed the Mn^{2+} was bound in the nuclease domain [32]. I tried approximately 700 premade conditions in an automated protein crystallization screening device. Three different crystallization conditions produced the crystals, and one condition was chosen to improve the crystal shape. The 15-well plates were used to optimize the crystallization conditions with the hanging-drop diffusion method manually. Finally, an optimized reservoir solution contained 2% (v/v) Tacsimate™ (pH 6.0), 0.1 M Bis-Tris (pH 7.0), and 18% (w/v) polyethylene glycol was obtained at 14℃. In the optimized condition, long rod-shaped crystals in the diffraction quality were obtained (Fig. 4).

For cryo-protection, the crystals in the drop were transferred to the viscous oil Paraton-N. Then the crystals were directly flash-cooled in liquid nitrogen. For data collection, Pohang Accelerator Laboratory (Pohang, Republic of Korea) 11C beamline was used at a wavelength of 0.97942 Å, and I finally collected the dataset with 93.8% completeness and 2.9 Å resolution (Fig. 5 and Table 2). The crystal lattice belonged to the primitive monoclinic space group, and the analysis of the diffraction along the h, k, l

axes further revealed a space group of $P2_12_12_1$, with cell dimension parameters of a = 72.9, b = 88.7, and c = 115.6 Å . The cell content analysis suggested that the asymmetric unit contained two protomers.

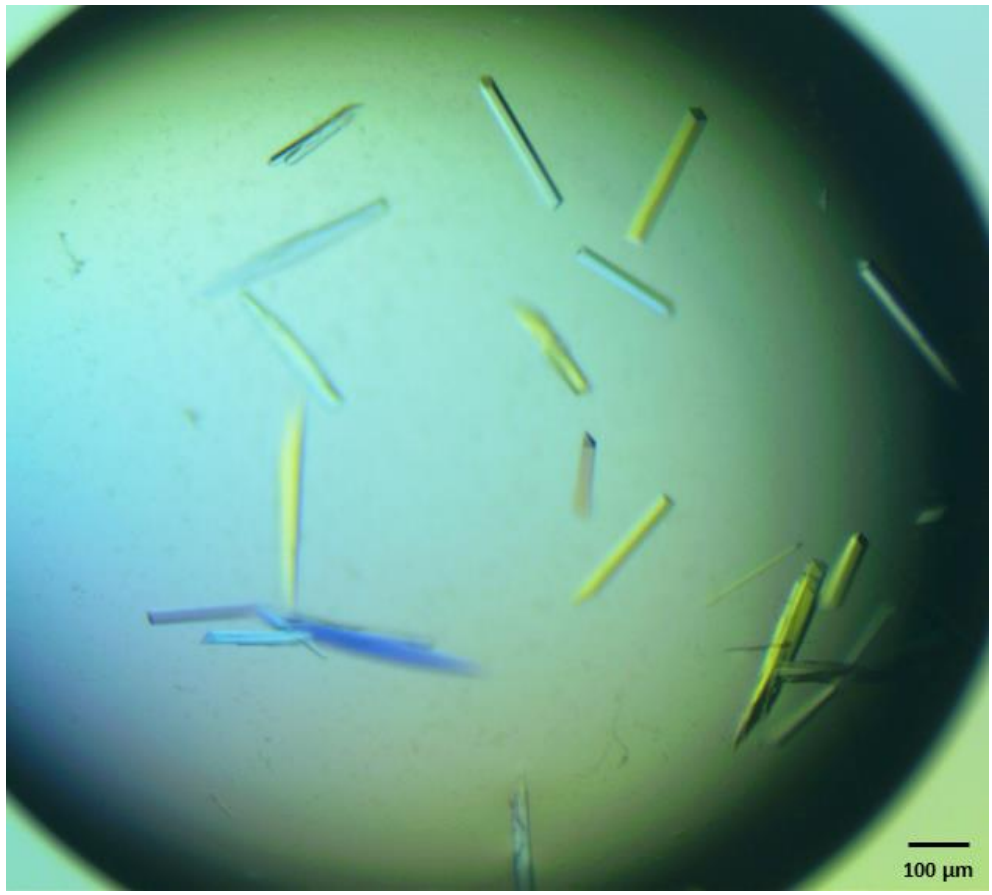

Figure 5. Crystals of the *S. aureus* SbcD-NCD protein

The approximate dimension of crystals is 0.03 x 0.03 x 0.25 mm.

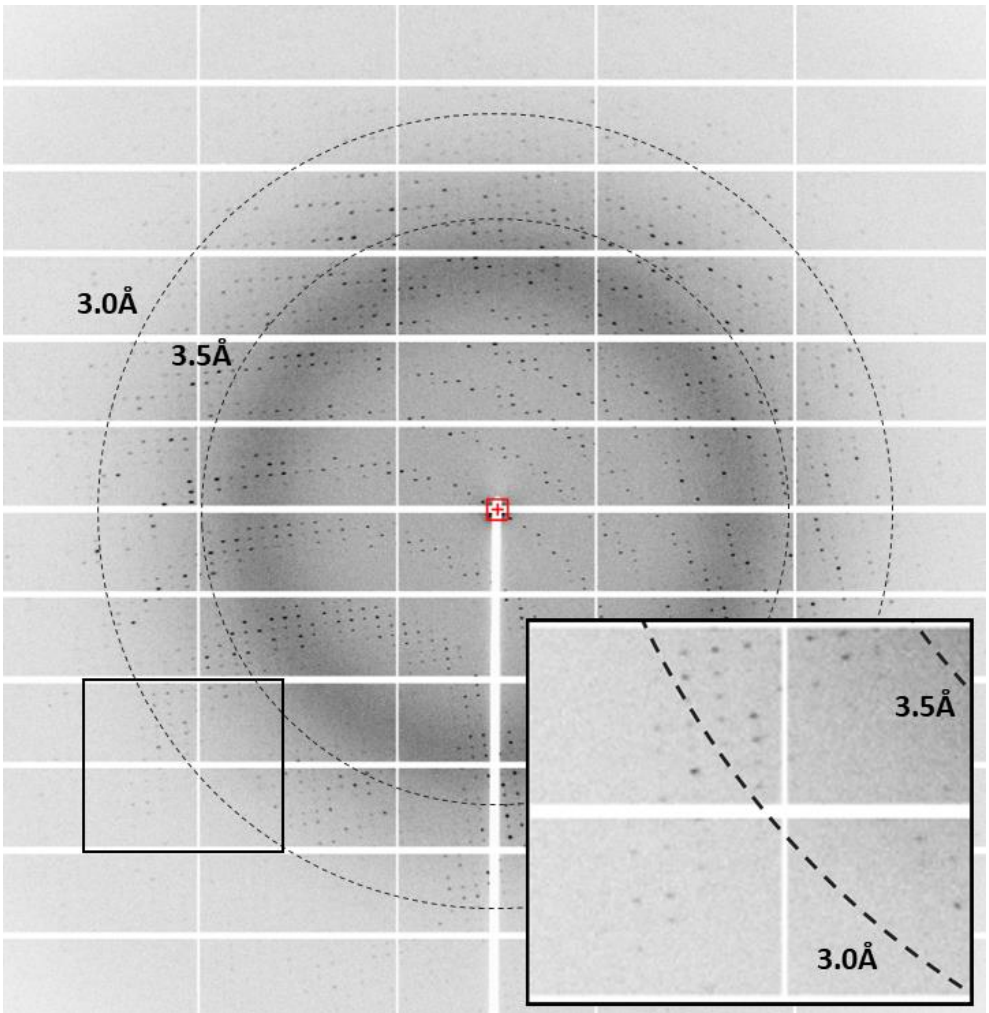

Figure 6. A representative diffraction image

The resolution circles for 3.0Å and 3.5Å are shown in dotted lines. A black rectangular area is enlarged in the right bottom corner.

Table 2. X-ray diffraction data

	SbcD-NCD
Data collection	
Beamline	PAL 11C
Wavelength (Å)	0.97942
Rotation range per image (°)	1
Total rotation range (°)	300
Exposure time per image (s)	1.5
Space group	$P2_12_12_1$
Cell dimensions	
a, *b*, *c* (Å)	72.9, 88.7, 115.6
β (°)	90
Resolution (Å)	50.0-2.90 (2.95-2.90)
Total No. reflections	16408
R_{merge}	0.148 (0.333)
High-resolution shell CC1/2	0.752
$I/\sigma I$	10.7 (3.5)
Completeness (%)	93.8 (86.7)
Redundancy	5.5 (3.5)

* The values in parentheses are for the highest resolution shell.

III-3. Overall protomer structure of SbcD-NCD

SbcD-NCD protomers are mainly composed of two domains named nuclease domain (residues 1-258) and capping domain (residues 265-320) which binding with SbcC. And two domains are connected by a flexible linker. SbcD-NCD protomers consist of 8 α-helices and 14 β-strands. There is an active site that cleaves DNA substrates on the top center of the nuclease domain (Fig. 7). The active site is exposed on the surface and two manganese ions are coordinated. The two protomers are dimerized by the interaction with two helices (α2-α3′, α3- α2′).

At the active site of SbcD-NCD, two manganese ions bind to Asp8, Asp48, Asn84, His10, His172, His210, and His212 (Fig. 8). The distance is about 2 angstroms on average and it is relatively strong. and the hydrolysis reaction occurs by the action of 2 manganese ions and 7 residues, resulting in cleavage of a phosphodiester bond between nucleotides. The SbcD-NCD forms a dimer by binding between helices (α2-α3′, α3- α2′). Among them, hydrophobic residues such as isoleucine, tyrosine, phenylalanine, tryptophan, and leucine form a hydrophobic core, forming a dimerization interface (Fig. 9).

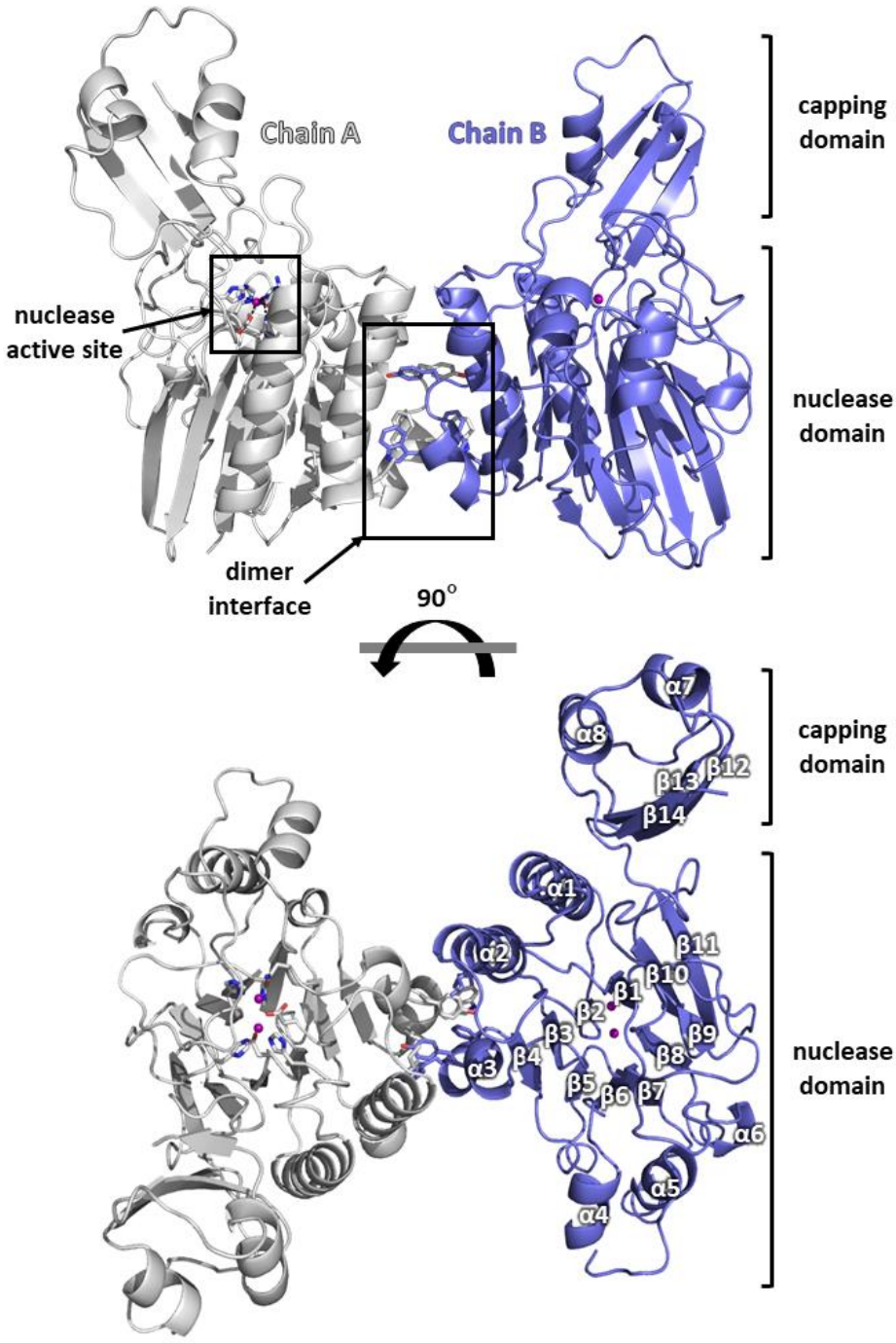
Chain A
Chain B
capping domain
nuclease domain
nuclease active site
dimer interface
90°
α7
α8
β13
β12
β14
α1
α2
β11
β10
β1
β2
β3
β9
β8
α3
β4
β5
β6
β7
α6
α5
α4

Figure 7. Dimer structure of SbcD-NCD in the ribbon representation

Ribbon representation of nuclease and capping domain of SbcD. Each domain and nuclease active site are annotated. α-helix and β-strand structures are labeled respectively. The asymmetric unit consists of a dimer, which is colored white and blue. Purple spheres represent Mn^{2+} ions. Two boxed areas with the black line are enlarged in Figure 8 and Figure 9.

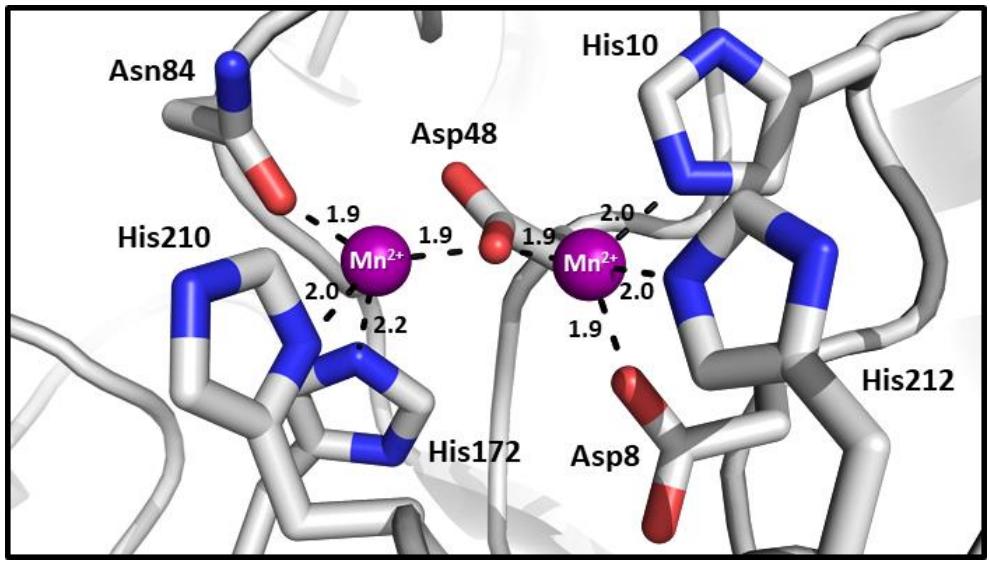

Figure 8. The active site structure of SbcD-NCD

This boxed area is enlarged from the nuclease active site in Figure 7. Core residues of nuclease active site of SbcD-NCD represent white stick with ribbon background. Two purple spheres indicate manganese ion. Interactions between two manganese ions and Asp8, His10, Asp48, Asn84, His172, His210, and His212 are shown in dotted lines. Distances are in Å.

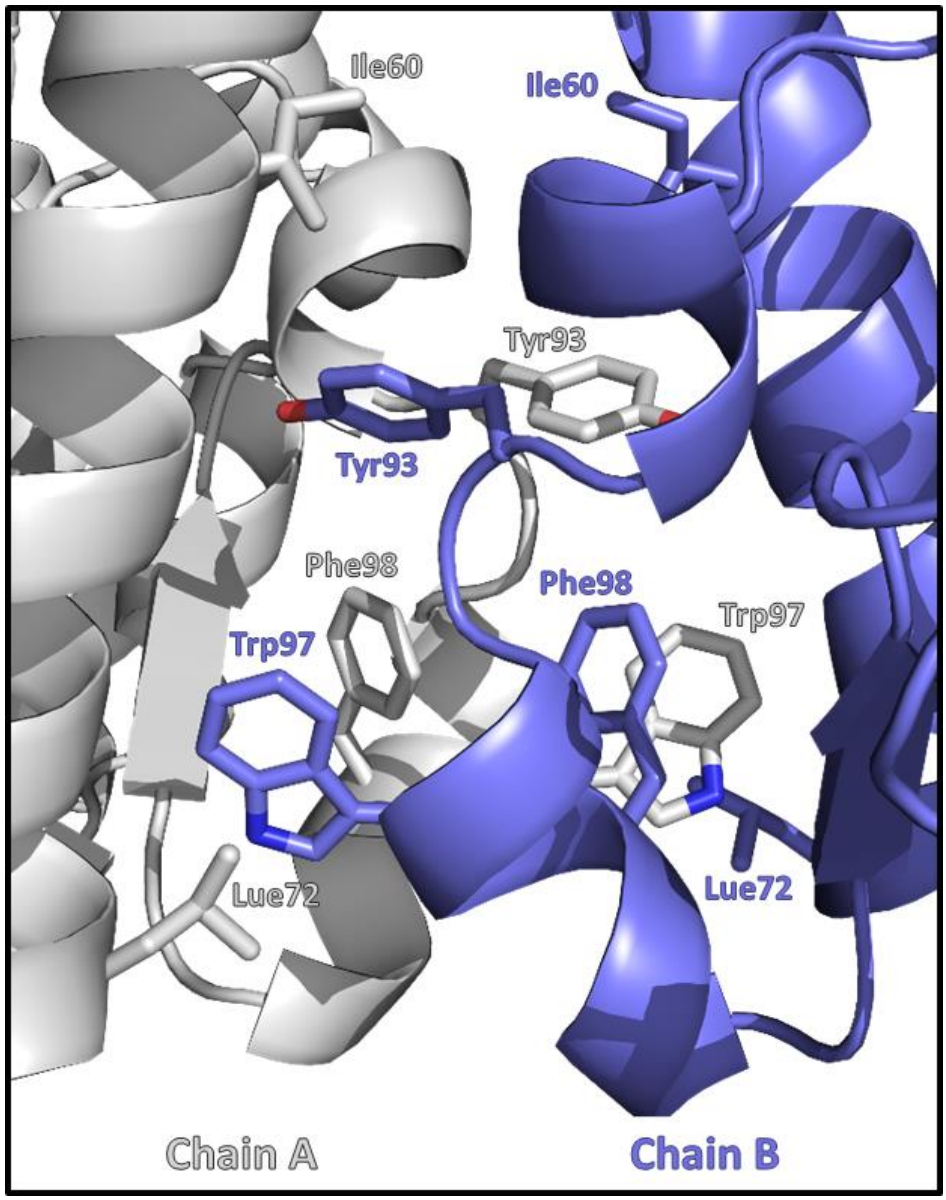

Figure 9. Hydrophobic interaction core in the SbcD-NCD dimerization interface

This boxed area is enlarged from the dimerization interface in Figure 7. 10 hydrophobic core residues in the dimerization interface are indicated and labeled in white and blue stick with ribbon diagram.

III-4. Structural comparison between *S. aureus* SbcD-NCD and *E. coli* SbcD-NCD

Structural comparison between *Sa*SbcD-NCD and *Ec*SbcD (PDB code 6s6v) shows that the nuclease and capping domains have a similar structure (Fig. 10). Comparing the active site of SbcD-NCD, it was confirmed that all seven important residues (Asp8, His10, Asp48, Asn84, His172, His210, His212) were conserved well (Fig. 11). However, the *Sa*SbcD-NCD protomers have a different dimeric interface in comparison with *Ec*SbcD (Fig. 10).

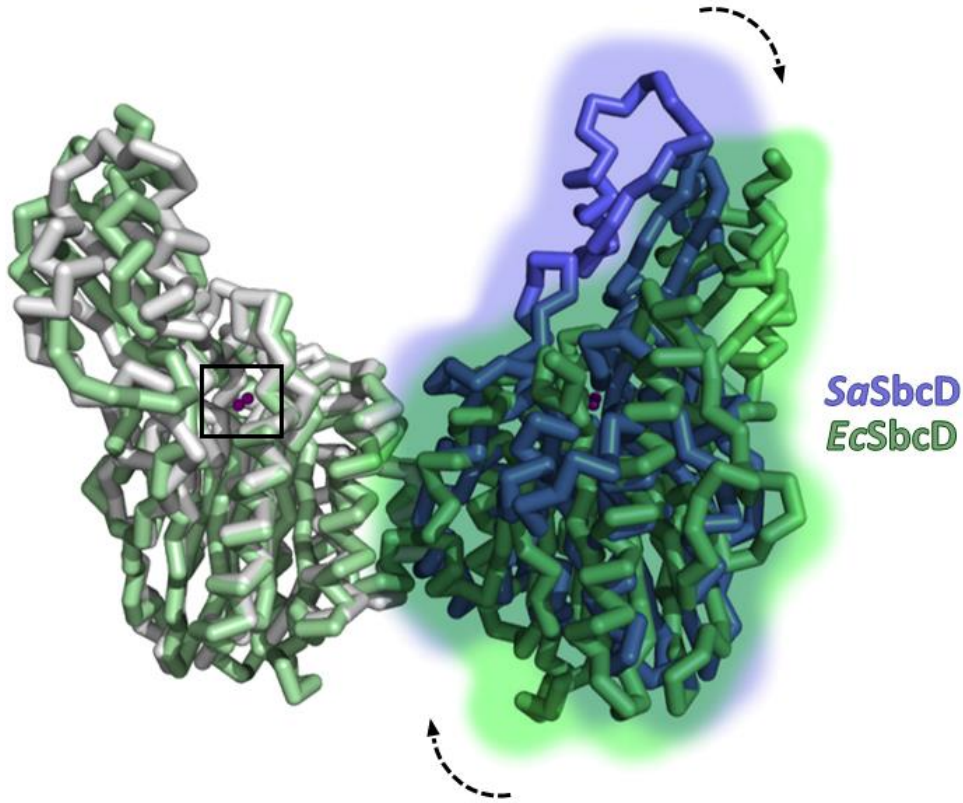

Figure 10. The overall structure of the *S. aureus* SbcD with *E. coli* SbcD

The dimer structure of the *S. aureus* SbcD-NCD (white and blue) is superimposed on E. coli SbcD (green, PDB code: 6s6v) in the ribbon representations. Dashed arrows indicate a conformational difference between *Sa*SbcD and *Ec*SbcD. The black rectangular region is enlarged in Figure 11.

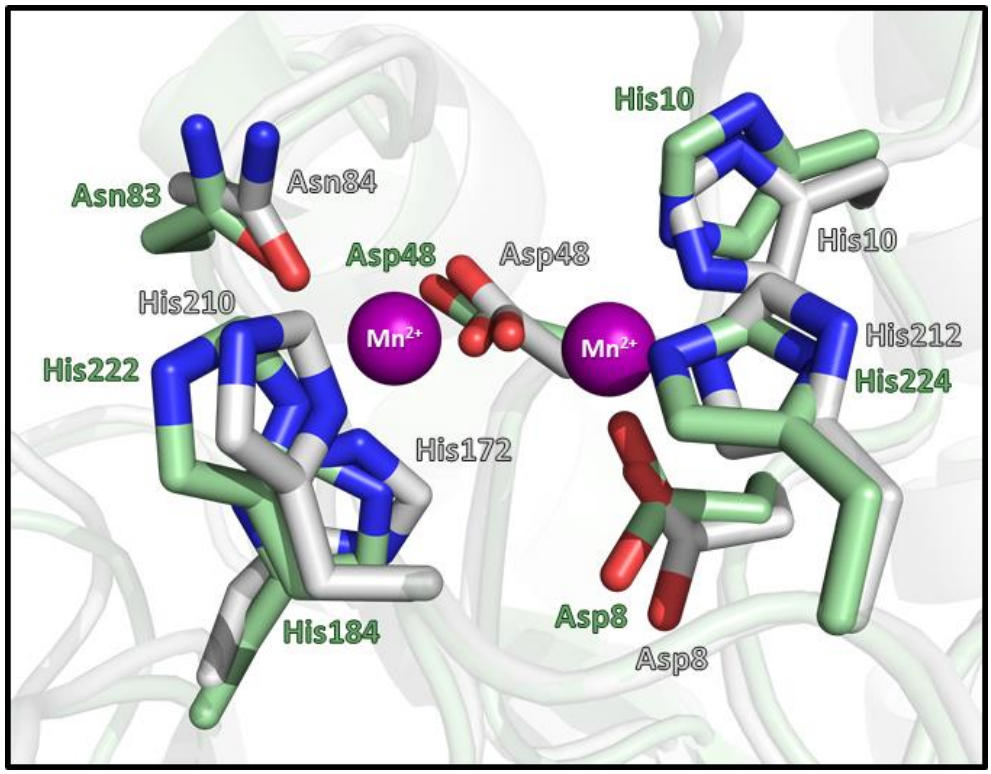

Figure 11. Comparison of *S. aureus* SbcD and *E. coli* SbcD at the active site

This boxed area is enlarged from the nuclease active site in Figure 10. Each residue of nuclease active site of *Sa*SbcD (white) and *Ec*SbcD (green, PDB code: 6s6v) is indicated and labeled in the stick representation with ribbon background. Two purple spheres represent manganese ion.

III-5. Endonuclease and exonuclease activities of the SbcD-NCD

Manganese for nuclease activity was added to 10 μM SbcD-NCD, and 500 ng of supercoiled DNA, linear DNA, and nicked DNA were reacted at 37 degrees for 60 minutes. As a result, SbcD-NCD showed nuclease activity to supercoiled DNA, linear DNA, and nicked DNA. In the case of supercoiled DNA, the endonuclease activity to make nicked DNA was shown, and linear DNA and nicked DNA showed exonuclease activity that degrades DNA (Fig. 12).

Supercoiled DNA was incubated as a substrate to observe endonuclease activity of SbcD-NCD at 37 degrees and at five different time points (0, 5, 15, 30, 60 minutes). Over time, the concentration of supercoiled DNA gradually decreased, and the concentration of nicked DNA increased. Nicked DNA was incubated as a substrate to observe exonuclease activity of SbcD-NCD at 37 degrees and at five different time points (0, 5, 15, 30, 60 minutes). It was observed that the nicked DNA was pulled downward over time and degraded gradually. (Fig. 13).

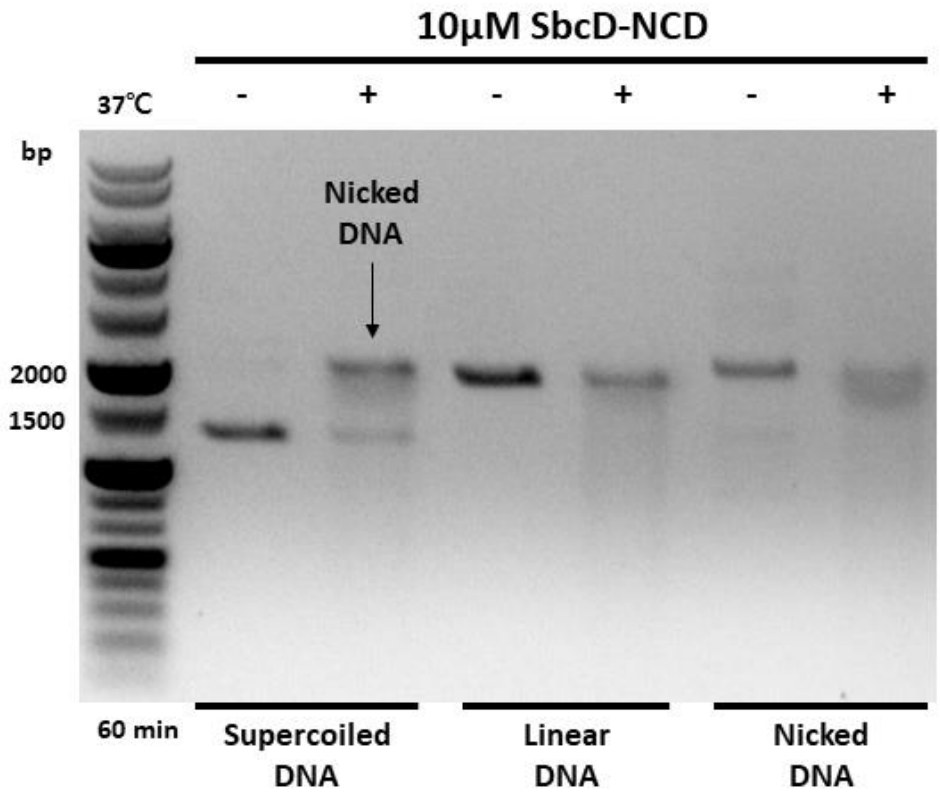

Figure 12. Nuclease assay of the SbcD-NCD

Nuclease assay of SbcD-NCD toward each dsDNA with Mn^{2+} at 37 degrees for 60 minutes. DNA ladder is shown in the left lane of agarose gel. The 1, 3, 5 lanes (from the left to the right) represent to control which is not contain SbcD-NCD (no enzyme).

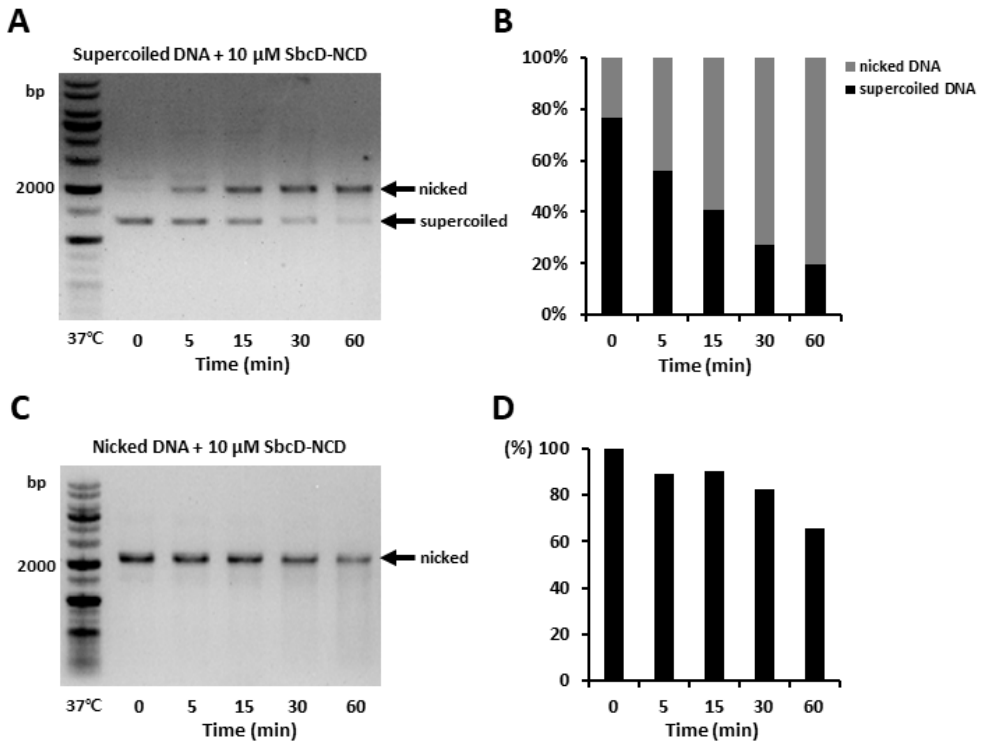

Figure 13. Endo-, exonuclease activity test of the SbcD-NCD

DNA ladder is shown in the left lane of agarose gel. Graphs quantifying the thickness of each band are shown on the right. **A.** Endonuclease assay of SbcD-NCD toward supercoiled DNA at 37 degrees for 0, 5, 15, 30, 60 minutes. **B.** Exonuclease assay of SbcD-NCD toward nicked DNA at 37 degrees for 0, 5, 15, 30, 60 minutes.

IV. Discussion

Since the DNA repair system is an important mechanism for living organisms, most species have a similar mechanism which is regulated by SbcCD (MRN) complex. Likewise, SbcD is conserved well in *S. aureus* Mu50 as well as other *staphylococcus* strains.

Structural and biochemical studies of SbcD have been mainly conducted in the *E. coli* system to reveal the molecular mechanism of the DNA repair process [10]. Compared with the SbcD of the *E. coli* (PDB code: 6s6v), all seven main residues binding to the manganese ion are conserved at the active site of *Sa*SbcD. It was thought that DNA cleavage occurred by the same nuclease mechanism with *Ec*SbcD in *Sa*SbcD, and the DNA substrate of the *Sa*SbcD was the same with *Ec*SbcD.

However, compared with the overall protomer structure of *Ec*SbcD-NCD, I observed that there was a difference in the dimer interface. The dimeric angle of *Sa*SbcD was slightly rotated compared to *Ec*SbcD (Fig. 10). The location of the capping domains differs, and this difference will appear to show substantial differences in interaction with the SbcC and interaction with the DNA substrate.

In previous studies, it was known that *Ec*SbcD cleaves circular single-strand DNA and blunt double-strand DNA as a substrate [10].

However, *Sa*SbcD-NCD had nuclease activity in supercoiled dsDNA, linear dsDNA, and nicked dsDNA. It was difficult that having both endonuclease and exonuclease activity in the structural aspect. Since the ends and middle of the DNA are structurally different, both of them will require a structural change of DNA or nuclease active site of SbcD.

*Sa*SbcD-NCD showed the endonuclease activity which nick supercoiled DNA. Since most of the DNA in bacteria is supercoiled [33], the nuclease activity of SbcD must be tightly regulated. It was anticipated that it would be possible to target a more specific DNA substrate in complex with SbcC [34].

Based on the structural and functional results of SbcD-NCD and SbcCD complex structure of *E. coli* [35] and *T. maritima* [24], I proposed the mechanism of how the SbcCD complex recognizes and cleaves DNA (Fig. 14). Two types of SbcCD complex structures were determined: closed-form (PDB code: 6s6v) and open form (PDB code: 3qg5). ATPase domain of SbcC bound each other in closed-form and separated in open-form. Thus, the nuclease active site was blocked by the ATPase domain in the closed-form, and the open-form is exposed from DNA. Conformational change from closed-form to open-form is expected to be induced by ATP hydrolysis, which will control nuclease activity [36]. SbcCD complex forms a huge hook by the long coiled-coil of SbcC in the closed-form [37]. In the open-form, the structure of the coiled-coil of SbcC is not determined. But

considering the structure, if the ATPase domain is folded to outsides, the coiled-coil hook will naturally descend. And if the DNA is in a coiled-coil hook, it will come down with the hook and fix between SbcD and coiled-coil. As a result, the DNA is located near the active site of SbcD, and the DNA will be cleaved by nuclease reaction.

In conclusion, the structure of *S. aureus* SbcD is important to investigate the DNA repair mechanism and its nuclease functions in the sterilization of bacteria. Although further study is required to explain the role of the SbcD in the DNA repair mechanism of *S. aureus*, this study contributes to understanding a molecular basis for how bacteria can resist sterilizing treatment. Further, it will help more effectively control the foodborne pathogens.

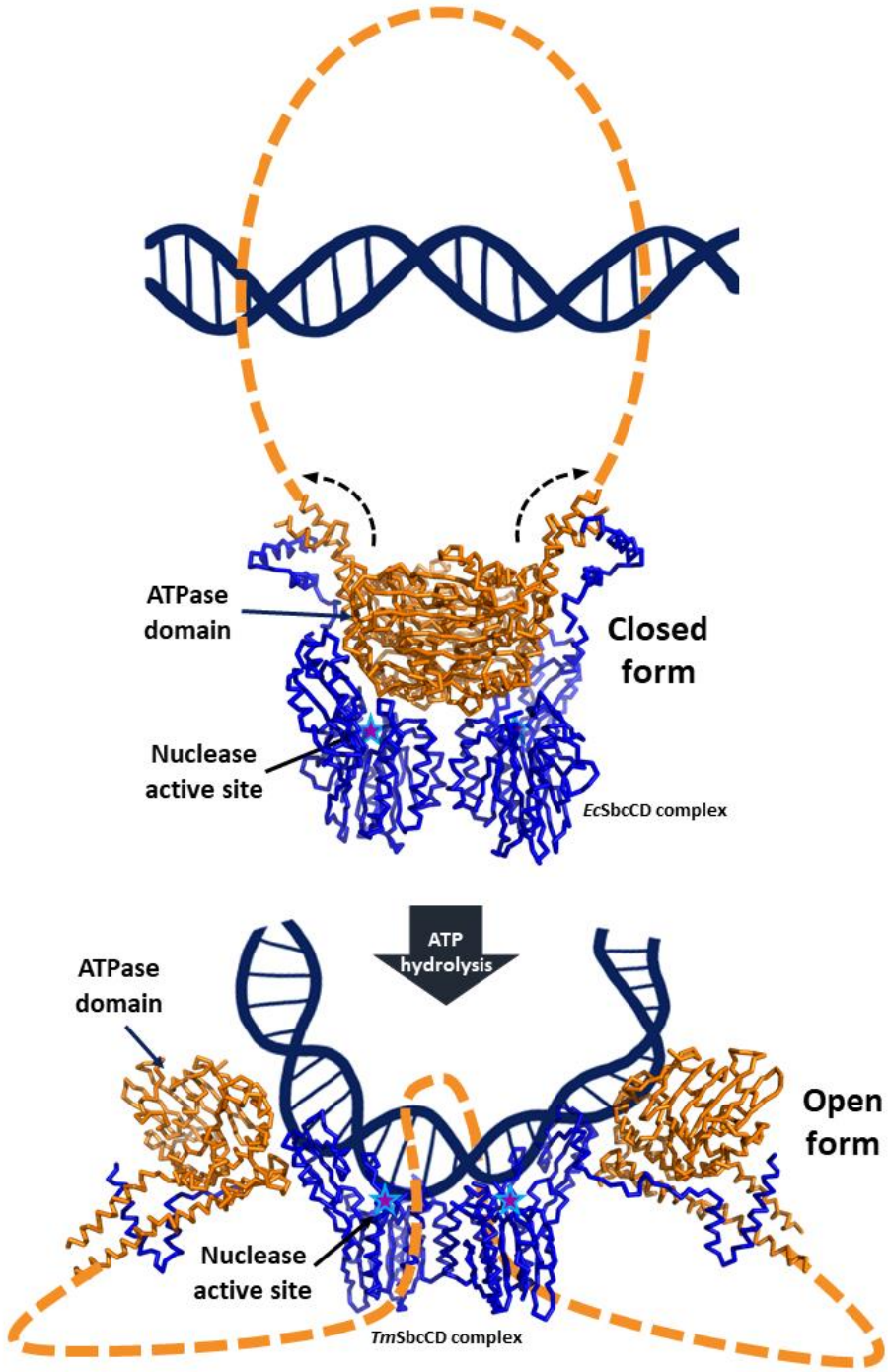
ATPase
domain
Closed
form
Nuclease
active site
EcSbcCD complex
ATP
hydrolysis
ATPase
domain
Open
form
Nuclease
active site
TmSbcCD complex

Figure 14. Proposed DNA recognition and cleavage mechanism of SbcCD complex

Proposed mechanism for ATP-dependent DNA recognition and cleavage by the SbcCD complex. SbcC (orange) and SbcD (blue) are depicted in the ribbon representation and the orange dotted line indicates a coiled-coil of SbcC. The purple star represents an active site of SbcD. Closed-form of *Ec*SbcCD complex (PDB code: 6s6v; top panel) and open-form of *Tm*SbcCD complex (PDB code: 3qg5; bottom panel) are showed with dsDNA. Dashed arrow indicates a conformational change by ATP hydrolysis between *Ec*SbcCD and *Tm*SbcCD.

V. Reference

1. Lowy, F.D., *Staphylococcus aureus infections.* New England journal of medicine, 1998. **339**(8): p. 520-532.

2. Bergdoll, M.S., *Staphylococcus aureus.* Journal of the Association of Official Analytical Chemists, 1991. **74**(4): p. 706-710.

3. Bhakdi, S. and J. Tranum-Jensen, *Alpha-toxin of Staphylococcus aureus.* Microbiology and Molecular Biology Reviews, 1991. **55**(4): p. 733-751.

4. Putnam, C.D., T.K. Hayes, and R.D. Kolodner, *Specific pathways prevent duplication-mediated genome rearrangements.* Nature, 2009. **460**(7258): p. 984-9.

5. Hanawalt, P.C., et al., *DNA repair in bacteria and mammalian cells.* Annual review of biochemistry, 1979. **48**(1): p. 783-836.

6. Sancar, A., et al., *Molecular mechanisms of mammalian DNA repair and the DNA damage checkpoints.* Annual review of biochemistry, 2004. **73**(1): p. 39-85.

7. Wigley, D.B., *Bacterial DNA repair: recent insights into the mechanism of RecBCD, AddAB and AdnAB.* Nature Reviews

Microbiology, 2013. **11**(1): p. 9-13.

8. Williams, R.S., J.S. Williams, and J.A. Tainer, *Mre11-Rad50-Nbs1 is a keystone complex connecting DNA repair machinery, double-strand break signaling, and the chromatin template.* Biochem Cell Biol, 2007. **85**(4): p. 509-20.

9. Wyman, C. and R. Kanaar, *DNA double-strand break repair: all's well that ends well.* Annu Rev Genet, 2006. **40**: p. 363-83.

10. Liu, S., et al., *Structural basis for DNA recognition and nuclease processing by the Mre11 homologue SbcD in double-strand breaks repair.* Acta Crystallogr D Biol Crystallogr, 2014. **70**(Pt 2): p. 299-309.

11. Lavin, M.F., *ATM and the Mre11 complex combine to recognize and signal DNA double-strand breaks.* Oncogene, 2007. **26**(56): p. 7749-58.

12. Lee, J.H. and T.T. Paull, *Activation and regulation of ATM kinase activity in response to DNA double-strand breaks.* Oncogene, 2007. **26**(56): p. 7741-8.

13. Stracker, T.H., et al., *The Mre11 complex and the metabolism of chromosome breaks: the importance of communicating and holding things together.* DNA Repair (Amst), 2004. **3**(8-9): p. 845-54.

14. Connelly, J.C., E.S. De Leau, and D.R. Leach, *DNA cleavage and degradation by the SbcCD protein complex from Escherichia coli.* Nucleic acids research, 1999. **27**(4): p. 1039-1046.

15. Connelly, J.C., E.S. de Leau, and D.R. Leach, *DNA cleavage and degradation by the SbcCD protein complex from Escherichia coli.* Nucleic Acids Res, 1999. **27**(4): p. 1039-46.

16. Connelly, J.C., E.S. de Leau, and D.R. Leach, *Nucleolytic processing of a protein-bound DNA end by the E. coli SbcCD (MR) complex.* DNA Repair (Amst), 2003. **2**(7): p. 795-807.

17. Lim, C.T., et al., *A novel mode of nuclease action is revealed by the bacterial Mre11/Rad50 complex.* Nucleic Acids Res, 2015. **43**(20): p. 9804-16.

18. Saathoff, J.H., et al., *The bacterial Mre11-Rad50 homolog SbcCD cleaves opposing strands of DNA by two chemically distinct nuclease reactions.* Nucleic Acids Res, 2018. **46**(21): p. 11303-11314.

19. Williams, R.S., et al., *Mre11 dimers coordinate DNA end bridging and nuclease processing in double-strand-break repair.* Cell, 2008. **135**(1): p. 97-109.

20. Hopfner, K.P., et al., *The Rad50 zinc-hook is a structure joining*

Mre11 complexes in DNA recombination and repair. Nature, 2002. **418**(6897): p. 562-6.

21. Hohl, M., et al., *The Rad50 coiled-coil domain is indispensable for Mre11 complex functions.* Nature structural & molecular biology, 2011. **18**(10): p. 1124.

22. Park, Y.B., et al., *Eukaryotic Rad50 functions as a rod-shaped dimer.* Nat Struct Mol Biol, 2017. **24**(3): p. 248-257.

23. Hopfner, K.-P., et al., *The Rad50 zinc-hook is a structure joining Mre11 complexes in DNA recombination and repair.* Nature, 2002. **418**(6897): p. 562-566.

24. Lammens, K., et al., *The Mre11:Rad50 structure shows an ATP-dependent molecular clamp in DNA double-strand break repair.* Cell, 2011. **145**(1): p. 54-66.

25. Diebold-Durand, M.L., et al., *Structure of Full-Length SMC and Rearrangements Required for Chromosome Organization.* Mol Cell, 2017. **67**(2): p. 334-347 e5.

26. Connelly, J.C., L.A. Kirkham, and D.R. Leach, *The SbcCD nuclease of Escherichia coli is a structural maintenance of chromosomes (SMC) family protein that cleaves hairpin DNA.* Proceedings of the National Academy of Sciences, 1998. **95**(14): p. 7969-7974.

27. Storvik, K.A. and P.L. Foster, *The SMC-like protein complex SbcCD enhances DNA polymerase IV-dependent spontaneous mutation in Escherichia coli.* Journal of bacteriology, 2011. **193**(3): p. 660-669.

28. Otwinowski, Z. and W. Minor, *Processing of X-ray diffraction data collected in oscillation mode.* Methods Enzymol, 1997. **276**: p. 307-26.

29. Winn, M.D., et al., *Overview of the CCP4 suite and current developments.* Acta Crystallographica Section D: Biological Crystallography, 2011. **67**(4): p. 235-242.

30. Emsley, P. and K. Cowtan, *Coot: model-building tools for molecular graphics.* Acta Crystallographica Section D: Biological Crystallography, 2004. **60**(12): p. 2126-2132.

31. Afonine, P.V., et al., *Joint X-ray and neutron refinement with phenix. refine.* Acta Crystallographica Section D: Biological Crystallography, 2010. **66**(11): p. 1153-1163.

32. Käshammer, L., et al., *Mechanism of DNA end sensing and processing by the Mre11-Rad50 complex.* Molecular cell, 2019. **76**(3): p. 382-394. e6.

33. Drlica, K., *Control of bacterial DNA supercoiling.* Molecular microbiology, 1992. **6**(4): p. 425-433.

34. Wilkinson, M., Y. Chaban, and D.B. Wigley, *Mechanism for nuclease regulation in RecBCD.* Elife, 2016. **5**: p. e18227.

35. Kashammer, L., et al., *Mechanism of DNA End Sensing and Processing by the Mre11-Rad50 Complex.* Mol Cell, 2019. **76**(3): p. 382-394 e6.

36. Lee, J.-H., et al., *Ataxia telangiectasia-mutated (ATM) kinase activity is regulated by ATP-driven conformational changes in the Mre11/Rad50/Nbs1 (MRN) complex.* Journal of Biological Chemistry, 2013. **288**(18): p. 12840-12851.

37. Wu, N. and H. Yu, *The Smc complexes in DNA damage response.* Cell & bioscience, 2012. **2**(1): p. 5.

VI. 국문초록

황색포도상구균은 대표적인 식품 매개 병원균으로 감염되면 식중독을 유발할 수 있다. 황색포도상구균의 감염을 예방하기 위해서는 식품에 가열, 자외선 조사, 차아염소산 처리와 같은 적절한 처리를 통해 살균해야 한다. 이런 살균 처리는 박테리아의 DNA에 손상을 입히는데 주로 DNA 이중 가닥 파괴를 유도하여 단백질의 발현을 억제하게 되고, 그 결과 박테리아가 사멸하게 된다. 하지만 박테리아는 이런 DNA 손상 스트레스에 저항하는 기작인 DNA 수선 기작을 갖고 있다. 황색포도상구균의 SbcCD 복합체는 DNA를 수선하기 위해 ATP-의존성 핵산 외부/중간 가수분해 활성에 의해 DNA 이중 가닥 파괴 부위에서 DNA 말단을 절단한다. 그 중 SbcD는 핵산가수분해 도메인, 캡핑 도메인 및 헬릭스-룹-헬릭스 도메인으로 구성되어 있다. SbcD의 구조 연구는 주로 그람 음성균에서 진행되었으며 그람 양성균에서는 아직 SbcCD 복합체의 구조가 규명되지 않았다. 또한, 박테리아 SbcCD 복합체의 작용 메커니즘을 분자 수준에서 설명할 수 있어야 한다. 본 연구에서는 그람 양성균인 황색포도상구균 유래의 SbcD 단백질을 과발현하고 정제하여 높은

순도의 고농도 단백질을 획득하여 구조 연구에 적합한 결정을 얻었다. X-선 회절 데이터는 2.9Å의 해상도로 수집되었고, SbcD 핵산가수분해 및 캡핑 도메인의 구조를 규명하였다. SbcD의 전체 구조를 보면 2 개의 망가니즈 이온이 SbcD의 활성 부위에서 발견되었고 7 개의 잔기에 결합되어 있었으며, 이는 대장균의 SdcD와 유사함을 보였다. SbcD-NCD 단백질에 의한 핵산가수분해 활성 실험은 슈퍼코일 DNA에 대한 핵산 중간 가수분해 활성과 선형 DNA 및 개방 된 원형 DNA에 대한 핵산 외부 가수분해 활성을 나타냈다. 구조 및 기작 결과를 바탕으로 SbcCD 복합체가 DNA 이중 가닥 파괴를 복구하는데 있어서 복합체의 활성을 어떻게 조절하는지에 대한 분자적 기작이 제시되었다. SbcD는 황색포도상구균뿐만 아니라 대부분의 박테리아에 보존되어 있는 DNA 수선 관련 단백질로 박테리아의 생존에 필수적이다. 식품 살균 과정에서 SbcD의 활성을 조절하는 것은 식품 살균에 대한 박테리아의 내성을 억제함으로써 식품 매개 병원균인 황색포도상구균을 제어할 수 있는 가능성을 제공할 것이다.

주요어: 황색포도상구균, 식품 매개 병원균, DNA 이중 가닥 파괴, DNA 수선, 핵산가수분해효소, 결정구조

학번: 2018-22430